Will carbon trading reduce spatial inequality? A spatial analysis of 200 cities in China

Article *in* Journal of Environmental Management · October 2022

DOI: 10.1016/j.jenvman.2022.116402

5 authors, including:

Yan Zhang
The Chinese University of Hong Kong

Nengcheng Chen
Wuhan University

Wang Siqi
China University of Geosciences

Mengtian Wen
Wuhan University

Highlights

Will Carbon Trading Reduce Spatial Inequality? A Spatial Analysis of 200 Cities in China

Yan Zhang,Nengcheng Chen,Siqi Wang,Mengtian Wen,Zeqiang Chen

- Geographical differences of the urban carbon emissions drivers.
- China national cross-city carbon trading industry will reach $153 billion.
- 131 net carbon absorbing cities, 144 net carbon emission cities.
- China's carbon emissions are still economically driven.
- Carbon trading markets have an positive impact on income equity.

Will Carbon Trading Reduce Spatial Inequality? A Spatial Analysis of 200 Cities in China

Yan Zhang[a], Nengcheng Chen[a,b], Siqi Wang[a], Mengtian Wen[a] and Zeqiang Chen[b,*]

[a] *State Key Laboratory of Information Engineering in Surveying, Mapping, and Remote Sensing, Wuhan University, Wuhan 430079, China*
[b] *National engineering research center of geographic information system, China University of Geosciences Wuhan 430074, China*

ARTICLE INFO

Keywords:
Carbon emissions
Carbon neutrality
Spatial justice
Urban sensing
Carbon markets
Emission trading scheme

ABSTRACT

The rising concentration of carbon in the atmosphere leads to increasing climate change, and it has become a worldwide consensus to reduce emissions. Considering the degree of economic development and industrial structure of different regions and the vast differences in the spatial distribution of clean energy reserves, it is essential to develop localized emission reduction programs. This study investigates the changes in city GDP after implementing carbon pricing policies. The results show that the carbon pricing policy could effectively reduce inequalities between "rich" and "poor" regions. The Moran index before and after the implementation of the policy decreases from 0.416 to 0.401. We also found spatial clustering patterns of carbon emissions, with the main drivers of carbon emissions differing significantly between developed and developing cities, resource-based and industrial cities, and southern and northern cities in China. The most crucial driver of carbon emissions is still the demand for economic development, which can explain more than 30% of carbon emissions. This study focuses on the impact of carbon market & carbon pricing on poverty alleviation and carbon reduction, makes up for the lack of "spatial justice" in the existing studies and provides a feasible carbon reduction plan for different cities.

1. Introduction

Due to rapid economic development, increasing industrialization, and a vast population base, China's demand for fossil energy is increasing. China surpassed the United States in 2006 and become the world's largest carbon emitter, emitting more than a quarter of the world's greenhouse gases (Fang et al., 2018). In the face of the growing environmental challenges, China has proposed the "carbon neutrality" and "emission peak" plans, increasing the retirement of high pollution and high energy consumption enterprises and accelerating the proportion of renewable energy (Mikovits et al., 2021). The plan is to reach the maximum value of carbon dioxide emissions by 2030, achieve a dynamic balance between carbon emissions and carbon absorption by 2060 (Guan et al., 2018; Zhao et al., 2017). The plan has been included in the government's 14th Five-Year Plan, which has become a national development strategy.

About 40 billion tons of CO_2 are emitted each year globally, 86% of which originate from fossil fuels and 14% from land use change (Londono-Pulgarin et al., 2021; Zhang et al., 2022d). These emissions are ultimately absorbed by land-based carbon sinks (31%) and oceanic carbon sinks (23%), with the remaining 46% remaining in the atmosphere (Fang et al., 2018; Chen et al., 2020a). In response to the combat climate change, carbon emission reduction has became the consensus of most countries. The specific actions include developing clean energy and promoting the construction of carbon trading market (Acheampong et al., 2022; Li et al., 2019).

The United Nations Framework Convention on Climate Change (UNFCCC) and the Paris Agreement both set a global target (as measured by law) to reduce greenhouse gas (GHG) emissions, to achieve net-zero emissions by the second half of this century, keeping global warming below $2°C$ (Nabernegg et al., 2019; Chen et al., 2020b). The list of countries that have implemented or partially implemented carbon pricing includes Argentina, Canada, Chile, China, Colombia, Denmark, the EU (27 countries), Japan, Kazakhstan, South Korea, Mexico, New Zealand,

*Corresponding author
cnc@whu.edu.cn (N. Chen); zeqiangchen@whu.edu.cn (Z. Chen)
grzy.cug.edu.cn/chenzeqiang (Z. Chen)
ORCID(s):

Norway, Singapore, South Africa, Sweden, the UK and Ukraine (Yang et al., 2022). Other countries being considered for membership include Brazil, Brunei, Indonesia, Pakistan, Russia, Serbia, Thailand, Turkey and Vietnam (Khosravi et al., 2020).

However, while there is an international consensus on carbon pricing policy, there are still two apparent inequalities behind global carbon emissions. First, the global elite (the top 10% of earners) account for 36% of global carbon emissions. In contrast, the extremely poor, who make up 12% of the global population, account for only 4% of global emissions (Semieniuk and Yakovenko, 2020). Moreover, due to the concentration of industry and population, cities, which cover only 2% of the global land area, house over 50% of the population, consume 75% of the energy and emit 85% of the Carbon dioxide (de Mendonca et al., 2021).

Exploring the impact of carbon markets on these two inequalities generated by carbon neutrality is of interest and is the main research question of this paper (Zhang et al., 2022e). As shown in Figure 1, the total electricity generation in mainland China is 7,218 TWh, and about 60% of the electricity comes from fossil fuels represented by coal, which is one of the mian sources of carbon emissions. In the meantime, China has abundant clean energy reserves, the actual exploitable wind energy resource reserves are 253 million kW, and the economically exploitable hydro energy is 402 million kW, which has a very high exploitation potential (Caineng et al., 2020; Dallaire et al., 2019; Linke et al., 2019). However, there is an apparent spatial "resource mismatch" for clean energy in China, as the southeast region, with 43% of the land area, is home to 94% of the country's population and most industrial. While the northwest region, with its abundant land resources (57% of the country's land area) and clean energy (Figure S8 a,d), is home to only 6% of the country's population.

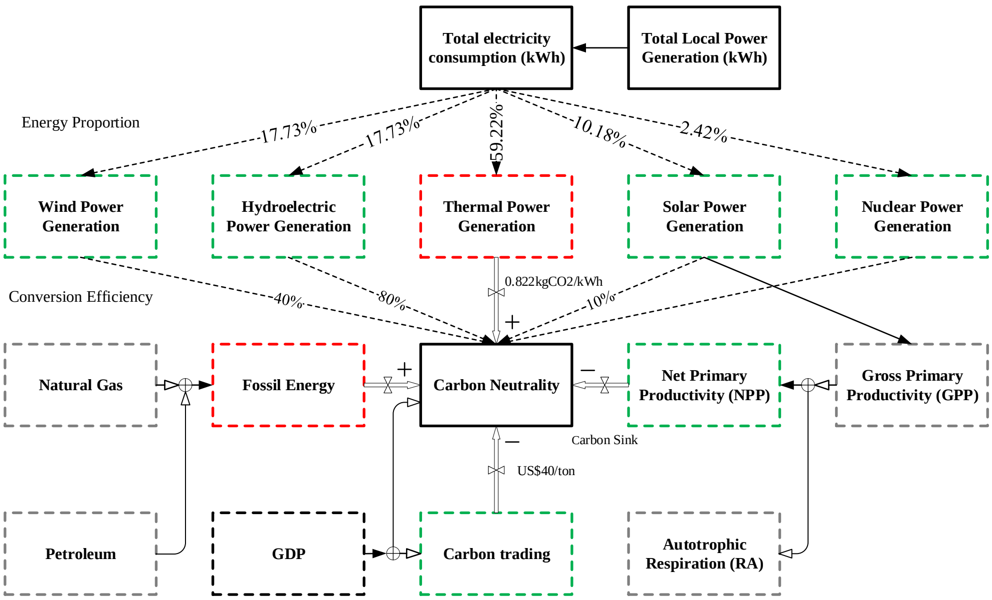

Figure 1: Carbon footprints and energy calculation framework (Green boxes represent a disincentive to carbon emissions Red boxes represent a contribution to carbon emissions)

Clean energy production, represented by photovoltaics, wind power, is not only unevenly distributed in spatial potential but also requires more land resources compared to fossil energy (Ristic et al., 2019; Xing et al., 2022). Developed regions of China (some large and prosperous cities) have scarce land resources and more energy needs. Less developed regions (some poor mountainous areas) have more abundant land resources, smaller populations, and less energy demand. This creates the problem of imbalance between the supply and demand of clean energy.

The Chinese government is actively promoting a carbon trading market to address this issue, being given two major tasks: carbon reduction and poverty alleviation. Developed regions can buy carbon emission rights from regions rich in renewable energy, and less developed regions can get more economic benefits from clean energy production (Opeyemi, 2021). It can solve the problem of tight urban land resources and promote spatial justice (a more equitable income distribution) (Zhu et al., 2020).

China first implemented the carbon Emission Trading System (ETS) (Chen and Lin, 2021; Guan et al., 2016) in eight regions and initially completed the construction of a national carbon trading market. Studies have already proven that carbon trading can effectively reduce carbon emissions (Yue et al., 2022; Liu et al., 2021). In addition, at the pricing of $40 per ton of CO_2 (Steckel et al., 2021), a massive industry of hundreds of billions of dollars will be created. In the context of carbon trading and carbon quotas, CO_2 emission rights can be regarded as develop rights to some extent. Big cities can purchase carbon rights to meet efficient resource use and high-yield industrial development (Chen et al., 2018; Yan et al., 2017). Similarly, a carbon pricing policy would use the market economy of free trade to eliminate inefficient, outdated capacity and "retire" highly polluting and energy-intensive industries (Zhao et al., 2022; Sun et al., 2021).

We conduct the following research around the impact of carbon pricing policy on poverty alleviation and carbon reduction.

1. Taking cities as research objects, we discuss which cities will benefit from carbon pricing policy at the national scale and whether it could reduce the spatial inequality.

2. Fusing multi-source urban sensing data, we construct a comprehensive carbon emission index, classify the main drivers of urban carbon emissions into four categories, and propose a clean energy development strategy according to local conditions.

2. Related Studies

Spatial justice refers to the fair and equitable distribution of socially valued resources and opportunities in the space (Soja, 2009, 2013). In this paper, "spatial justice" refers to the rational allocation carbon emission targets in the form of markets, both to promote carbon reduction and to bridge the gap between rich and poor (Sun et al., 2022; Brent et al., 2020). It requires guaranteeing equal and free opportunities for economic and social development for all people (Zhang et al., 2022b).

The inequity of the existing carbon emissions pattern in the introduction has been discussed extensively. Urbanization has brought spatial justice issues, including inequality in public services (Li et al., 2022), unequal distribution of resources and uneven regional development (Chao, 2019; Uwayezu and De Vries, 2018). In the context of energy security, the concept of energy justice has been proposed, but spatial inequalities are not considered. It defines "energy justice" as a global energy system that fairly distributes both the benefits and burdens of energy services and one that contributes to more representative and inclusive energy decision making (Sovacool et al., 2017). As clean energy sources gradually replace fossil energy, more and more scholars are discussing social justice in the context of sustainable energy transition (Cheng et al., 2022); environmental justice in the context of clean energy development (Avila, 2018); the tendency of low carbon interest coalitions to deprive vulnerable social groups of assets to maximize their benefits; and the risk of fuel poverty to the poor in energy decarbonization (Sovacool et al., 2019). Because of the further implementation of the carbon pricing policy, the original measure of economic development in terms of GDP is no longer suitable (Vaninsky, 2021). Some researchers have started to focus on the energy efficiency of economic development, promote the growth of green GDP, propose the concept of "Clear waters and green mountains are as good as mountains of gold and silver"(Amri, 2017). In this case, gross ecosystem product is born, calling on the government to make decisions from the perspective of ecosystem assets (Ouyang et al., 2020).

There are still some shortcomings in the existing studies.First, the spatial scale of the analysis is large, mainly using provinces as spatial units (Liu et al., 2022). Second, the impact of carbon trading policy (carbon tax) on carbon reduction has been well analyzed (Zhang et al., 2022a; Wang and Su, 2020), but the impact of this policy on poverty alleviation is still need to be studied. In order to study the impact of carbon pricing policies on spatial justice after their implementation, we discuss the different driving factors of CO_2 emissions in spatial terms and explore the spatial variation of city "net" GDP per capita after carbon trading (Wang et al., 2022b).

3. Study Method

3.1. Data selection and data sources

In the data preparation, we try to fuse multiple data sources, including city statistical yearbooks, remote sensing, inversion of sensor network data, ecological measurements (Zhang et al., 2021b,a), etc. Besides,we referred to the relevant literature and selected the appropriate carbon emission indicators as many as possible, including regional economy (Wu and Xie, 2020), industrial development level (Liu et al., 2019), education level (Wang et al., 2020),industrial structure(Zhang et al., 2020), urbanisation level (Zhou et al., 2019), technology innovation and technological progress (jiemin and chen, 2022). In addition, existing studies also confirm the strong correlation between night-light remote sensing and carbon emissions, so we also include it (Zhang et al., 2022d,c).

We use principal component analysis (PCA) to analyze these elements and construct carbon footprint evaluation indicators. As shown in Tabel S6 , these indicators include Water Resource (WR), Wind energy potential (WEP), Solar energy potential (SEP), Carbon Sequestration (CS), Net Primary Productivity (NPP), Public Budget Revenue (PBR), Sulphur Dioxide Emission (SDE), Nitrogen Dioxide Emission (NDE), Industrial Soot Emission (SE), Liquefied Petroleum Gas Supply (LPGS), Annual Electricity Consumption (AEC), Gas Supply (GS), Luminous remote sensing image brightness values (LRS), Water Supply (WS), and dozens of other urban indicators. Among them, the urban CO_2 emission data are estimated using IPCC guidelines [1] and energy statistics yearbook (Shan et al., 2020, 2018).

Because the COVID-19 has a significant economic impact on the world in 2020, we uniformly selected data from 2018-2019 for the analysis. To ensure the accuracy of the data, we did not use mean or zero values to supplement the missing and did not include cities with these fields missing in the calculation. After data cleaning and data pre-processing, 197 cities out of 371 cities in China have complete data and are our main analysis target.

Figure S8 illustrates the spatial distribution of the resource supply side (subplots a,d) and resource consumption side (subplots b,c,e,f) in China. Since the distribution of hydropower potential is difficult to assess at the spatial scale of administrative divisions, we focus on biomass, solar (Figure S8a, based on an average annual operation of 1,400 hours), and wind (Figure S8d, based on an average annual operation of 2,000 hours) to assess the clean energy potential (Hernández et al., 2020) at the spatial scale of prefecture-level cities.

3.2. Data pre-processing and comprehensive index construction

We normalized the data firstly, if the indicator positively affects carbon emissions (e.g., secondary industry size), the formula corresponding to the positive indicator is used. Similarly, the indicator negative affects carbon emissions (e.g., plant carbon sink) was regarded as negative indicator. Afterwards, a comprehensive carbon emission index was constructed using PCA.

$$X'_{ij} = \begin{cases} \frac{X_{ij} - \min X_j}{\max X_j - \min X_j}, \text{Positive indicators} \\ \frac{\max X_j - X_{ij}}{\max X_j - \min X_j}, \text{Negative indicators} \end{cases} \tag{1}$$

Where,X'_{ij} is the standardized result of the ith data of the jth index, and $\min X_j$,$\max X_j$ are the maximum and minimum values of all data in the jth index, respectively.

The basic idea of PCA is to derive a few principal components as composite indicators from the original multi-indicator variables. The composite indicators can contain most of the information of the original multiple indicators and are independent of each other. In the comprehensive evaluation of multiple indicators, the use of PCA can determine the weights, makes the evaluation results objective and comprehensive.

In the urban carbon emission driver analysis, n indicators X_i constitute a vector $X = \left(X_1, X_1, \cdots, X_n\right)$ for evaluating cities. PCA linearly combines these observed indicators X_i to form a new composite indicator F_i that satisfies the following transformation:

$$\begin{aligned} & F_i = a_{i1}X_1 + a_{i2}X_2 + \cdots + a_{im}X_n, \\ & i = 1, 2, \cdots, k \end{aligned} \tag{2}$$

where,X_i is the ith indicator ($i = 1, 2, ..., m$); F_j is the jth principal component; a_{ij} corresponds to the jth component of the eigenvector of the ith eigenvalue; k is the number of principal components; m,n is the number of indicators, n represents all the indicators, m represents the retained indicators, in this paper $m = n$. We calculate the composite index (CI) by multiplying the variance contribution of the principal components ω_i by the F_i score of each principal component.

[1] www.ipcc.ch

$$
\begin{aligned}
&CI = F_1\omega_1 + \cdots + F_i\omega_i + \cdots + F_k\omega_k \\
&\omega_i = \frac{\lambda_i}{\sum \lambda}
\end{aligned}
\tag{3}
$$

3.3. Spatial autocorrelation and spatial regression

Spatial autocorrelation reflects the degree of correlation between regional units. It is a spatial statistical method to detect and quantify the spatial dependence. The spatial autocorrelation theory suggests that the closer things are to each other, the more similar they are. When the attribute value of a sample point is high (low), and its neighbourhood is also high (low) , it is called positive correlation; the opposite is called negative correlation.

Spatial autocorrelation includes both global and local indicators. The global indicator is used to detect the spatial pattern of the whole study area, using a single value to reflect the degree of autocorrelation in the area. The local indicator calculates the degree of correlation between each spatial unit and its neighbouring units concerning a particular attribute.

The global Moran index I, calculated using the following equation:

$$
I = \frac{n\sum_{i=1}^{n}\sum_{j=1}^{n} w_{ij}\left(x_i - \bar{x}\right)\left(x_j - \bar{x}\right)}{\sum_{i=1}^{n}\sum_{j=1}^{n} w_{ij}\sum_{i=1}^{n}\left(x_i - \bar{x}\right)^2} = \frac{\sum_{i=1}^{n}\sum_{j\neq i}^{n} w_{ij}(x_i - \overline{x})(x_j - \overline{x})}{S^2\sum_{i=1}^{n}\sum_{j\neq i}^{n} w_{ij}}
\tag{4}
$$

The local Moran index can reveal spatial relationships that are masked by the global index, which is calculated as follows:

$$
\begin{cases}
I_i = \dfrac{x_i - \bar{X}}{S_i^2}\displaystyle\sum_{j=1, j\neq i}^{n} w_{i,j}\left(x_j - \bar{X}\right) \\
S_i^2 = \dfrac{\sum_{j=1, j\neq i}^{n}\left(x_j - \bar{X}\right)^2}{n-1}
\end{cases}
\tag{5}
$$

Where n is the total number of data; x_i is the weighted value of the ith sample; $\bar{X}$ is the mean of the weighted Spatio-temporal network kernel density estimates; and $w_{i,j}$ is the spatial weight between sample i and sample j. The local Moran index is also known as the Local Indicators of Spatial Association (LISA) test.

The "hot cities" or "cold cities" of carbon emissions can form clusters (spatial clusters) or exist individually (spatial outliers) in space (Pravitasari et al., 2018; Wang et al., 2022a). We can suggest reasonable carbon emission based on the spatial clustering of different principal component indicators F_i.

The general equation of the spatial regression model is as follows:

$$
\begin{cases}
Y = \rho W_1 + \beta X + \mu \\
\quad \mu = \lambda W_2 + \varepsilon
\end{cases}
\tag{6}
$$

Where Y is the predicted urban CO_2 emissions, X is the value of the constructed indicator system F_i, ρ, β is the spatial regression coefficient, W is the spatial weight matrix, μ is the residual term, λ is the regression coefficient of the residual term, and λ is the random error. When $\rho = 0$ and $\lambda = 0$, the equation is expressed as an ordinary linear regression equation (OLS). When $\rho \neq 0$, $\beta = 0$, and $\lambda = 0$, the one-order spatial regression model is obtained. When $\rho = 0$, $\beta \neq 0$, $\lambda \neq 0$, we get Spatial Error Model (SEM). In this paper, the spatial weights are constructed based on the one-order Queen adjacency matrix.

In addition, we can use the global Moran index to assess the spatial distribution of "green GDP"(GDP net of carbon tax) of Chinese residents before and after the policy implementation. In addition, based on the comprehensive carbon emission index system constructed in the previous section, we can also use spatial regression to analyze the main drivers of carbon emissions in cities to explain the question of "because of what carbon emissions".

4. Experimental results and discussion

This section is divided into three main steps. First, we explore whether poor regions could obtain benefits under carbon trading policy, whether could bring income equity, how the spatial distribution of national GDP per capita changes before and after the implementation of this policy. This part of the work will help assess the pro-poor effects of carbon trading. Second, we discuss the main drivers of carbon emissions in different types of cities and the characteristics of their spatial distribution, and this part of the work will help to develop reasonable policies for emission reduction. The final step combines the above two steps, and we fit urban CO_2 emissions based on a system of indicators and SEM.

4.1. Impact of carbon trading on Spatial Justice

Based on the following five ideal conditions, we have made a conservative calculation of urban carbon accounts.

1. A well-constructed nationwide carbon trading market, with carbon prices fluctuating around $40 per ton (actually, the current carbon price is lower in China and higher in Europe, so we take the average value of $40).

2. Based on the existing clean energy development, each city develops 0.01% of the potential clean energy. In other word, it is assumed that we add 0.01% of urban land resources are used for clean energy development. Wind energy (2,000 hours of effective power generation per year) and solar energy (1,400 hours of effective power generation per year) (**?**Qiu et al., 2022) have different power generation efficiencies in different regions (Figure S8 a,d).

3. All energy consumption are uniformly converted into CO_2 for calculation (thermal power plants consume 0.33Kg of standard coal and emit 0.822Kg of CO_2 for every 1kwh of electricity produced on average (Wang et al., 2021b)). For example, an increase of 1kwh of clean energy means an emission reduction of 0.822Kg of CO_2. The annual CO_2 emissions of the city minus the annual carbon sequestration (carbon sink) and the carbon reduction under condition 2 is the net CO_2 emissions of the city.

4. Every company and individual needs to compliancea carbon neutral policy. The excess CO_2 emissions after the calculation of condition 3 need to be compensated by purchasing carbon rights (imposing carbon taxes). The purchaser is the city's producer or government, and the carbon tax will actually be passed on to local residents.

5. The existing energy consumption will not increase or increase a little, and promote the replacement of clean energy to traditional fossil energy (such as the development of new energy electric vehicles, gradually phase out coal-fired power plants, etc.).

In the last, the "net" GDP per capita after carbon trading could be calculated as follows [2]:

$$\begin{aligned} Carbon\ Emissions - Carbon\ Sequestration - Carbon\ Reductions &= Traded\ Carbon\ Emissions \\ Net\ City\ GDP = City\ GDP - Traded\ Carbon\ Emissions \times Carbon\ Pricing & \end{aligned} \tag{7}$$

After our calculations, if the above 5 more conservative conditions are met, China will still emit 227.989 million tons of carbon dioxide into the atmosphere each year, a figure that has been greatly reduced compared to the existing carbon emissions. Although China's industrialization has not yet stopped and CO_2 emissions are still increasing. However, we only consider new wind and light energy in our calculations, and do not consider new nuclear and hydro energy development, and some cities in the west with high potential for clean energy development have not collected data. Therefore, under the above conditions, it is possible to achieve the goal of carbon neutrality by 2060 with roughly stable CO_2 emissions and the orderly development of clean energy sources.

The detailed calculations are shown in Table S7 . The national cross-city carbon trading would reach an industry size of 973.283 billion yuan ($153 billion). As shown in Figure 2, there are 131 cities in China that are "net carbon absorbing cities", and about 537 million people will benefit from this, with an average gain of about 1707 yuan ($268) per person/year. This benefit is likely to be in the form of a surplus from carbon trading, which will eventually be reflected in the city's GDP. Conversely, 144 cities are "net carbon emission cities" and will pay an additional carbon

[2] City carbon emissions are calculated according to IPCC standards (www.ipcc.ch).

tax. Approximately 696 million people will incur an additional cost of 1,398 yuan ($219) per person per year as a result of the carbon tax. This part of the cost may be passed on by local factories to local consumers and will also be reflected in the city's GDP.

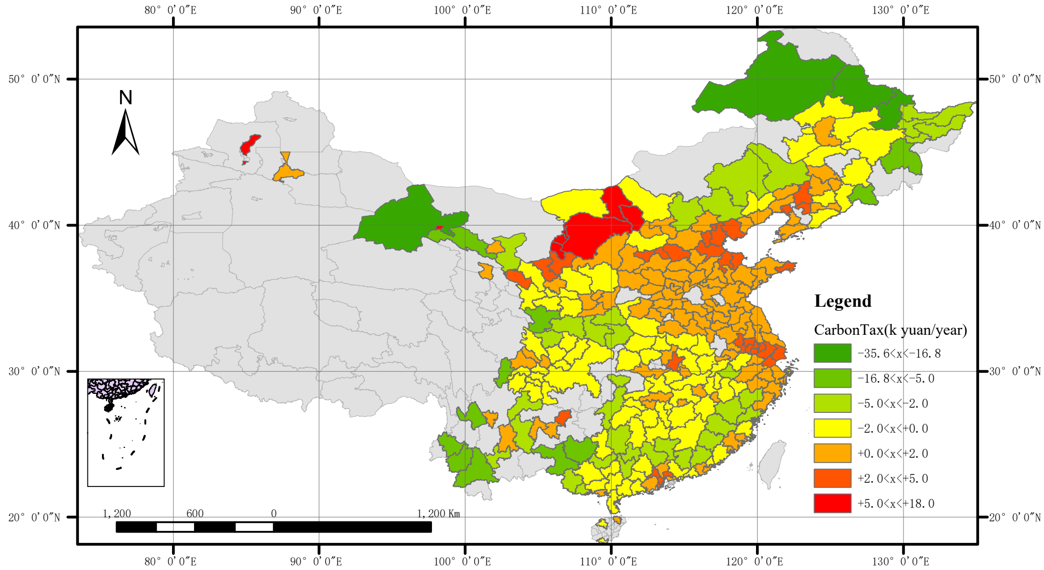

Figure 2: Spatial distribution of the carbon tax to be paid by each city in China (the greenish color represents carbon surplus, the redish color represents carbon deficit, and the different colors indicate the amount of carbon tax the city needs to pay per capita).

Figure 2 shows the carbon tax imposed on different cities due to carbon trading policies. The existing city GDP after deducting the carbon tax to get the "net" city GDP.

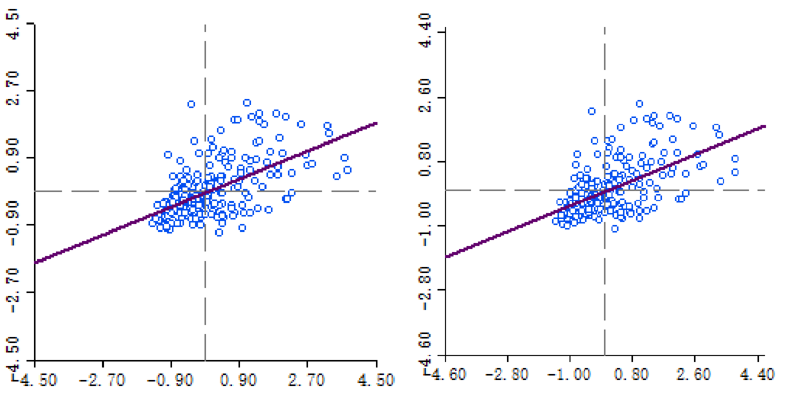

(a) Before carbon pricing $Moran's\ I = 0.416$ (b) After carbon pricing $Moran's\ I = 0.401$

Figure 3: Measuring the spatial auto-correlation of GDP per capita (The x-axis represents urban GDP per capita, the y-axis represents the spatial lag calculated based on Equation 5 and Geoda 1.20 software.)

Figure 3 illustrates the spatial autocorrelation of per capita GDP in Chinese cities before and after the implementation of the carbon pricing policy. The carbon market can significantly reduce the spatial disparity in income distribution (at the $p < 0.05$ confidence level). The Moran index of urban GDP per capita in China decreases from

0.416 to 0.401 under the not-aggressive clean energy development measure. It implies that relatively backward regions can gain through carbon trading, bridging the income gap between urban-rural, developed and backward regions and addressing the inequality of carbon emission rights.

Besides, we used T-distributed Stochastic Neighbor Embedding (T-SNE, which has proven to be a suitable method for high-dimensional data processing, to convert the similarity between data points into probability (Van der Maaten and Hinton, 2008; Chen et al., 2021)) dimensionality reduction method to obtain the distribution states of all cities (14 city indicators mentioned in 3.1) on a two-dimensional space (Figure 4).

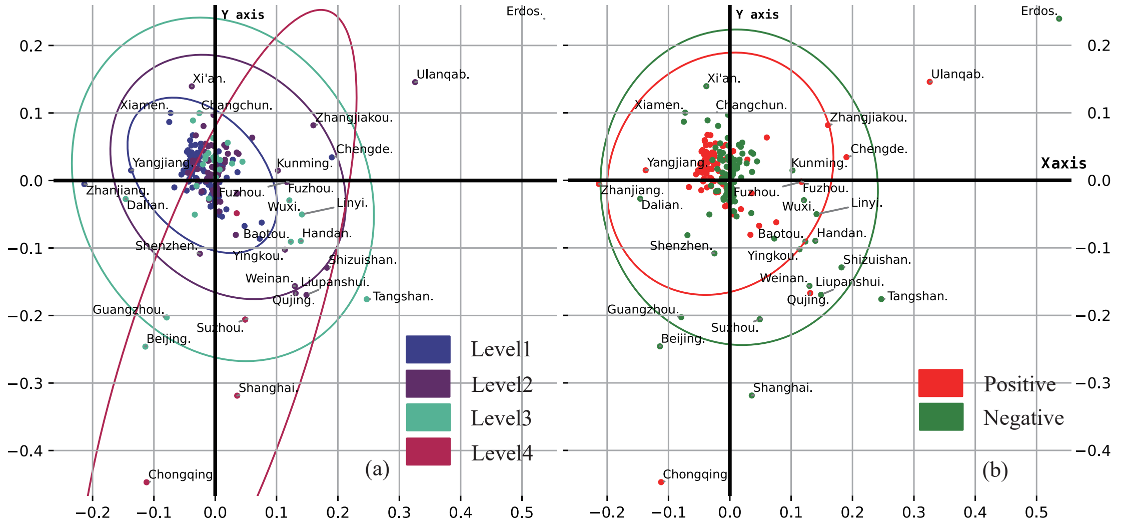

Figure 4: T-SNE reduced dimensional presentation of cities with confidence ellipse distribution (a indicates the intensity of carbon emissions in different cities, and are categorised into 4 levels from low to high; b indicates whether the city benefits or loses from carbon pricing/carbon markets, i.e. positive vs. negative cities)

Figure 4 b shows the positive and negative cities after the implementation of the carbon pricing policy. The T-SNE dimensionality reduction algorithm allows us to distinguish between cities that have benefited from carbon pricing (positive, more clean energy or higher carbon sequestration capacity), primarily located in the second quadrant of the Figure. The dimensionality reduction method could give us a good understanding of the data set, and we plot the confidence ellipse of the data (Schubert and Kirchner, 2014). It shows that most of the cities are in similar positions after the dimensionality reduction. There is no significant difference in the distribution of indicators between the group of positive cities and the group of negative cities. Figure 4 a, on the other hand, shows the complexity in terms of total urban carbon emissions. We use the natural breakpoint classification to classify cities into four classes based on carbon emissions from small to large. The fact that cities with significant carbon emissions differ significantly from the ordinary city in some indicator dimensions suggests that urban carbon emissions are affected by the compounding of multiple factors across multiple indicators. We analyze this compounding effect of urban carbon emissions in the next section.

4.2. Major drivers of urban carbon emissions and Spatial justice differences

The second part analyses the causes of carbon emissions in Chinese cities and evaluates the inequality in the distribution of the main drivers in a spatial perspective. Fourteen indicators related to carbon emissions shown in Figure 5 are selected. Firstly, we standardize the data. We consider those indicators that can make the city carbon emission decrease as negative indicators and those that increase the city carbon emission as positive indicators to study the driving factors of urban carbon emission. Figure 5 also shows the correlation between the standardized indicators and the linear fit results.

In order to avoid too much of a personal and subjective component during the construction of the evaluation system. We conducted a principal component analysis of these indicators using SPSS Statistics 25 software and extracted four principal components, as shown in Table 1. They can explain 34.909%, 26.705%, 15.916% and 8.264% of the variance of the original data, respectively, for a total of 85.794% of the original information. The Kaiser-Meyer-Olkin value for

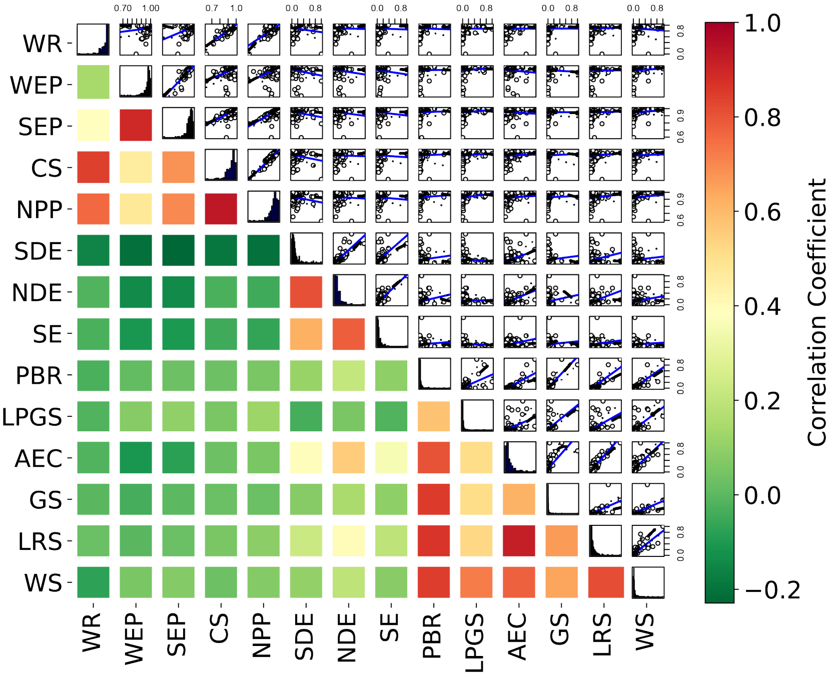

Figure 5: Correlation of indicators and linear fitting results (Water Resource (WR), Wind energy potential (WEP), Solar energy potential (SEP), Carbon Sequestration (CS), Net Primary Productivity (NPP), Public Budget Revenue (PBR), Sulphur Dioxide Emission (SDE), Nitrogen Dioxide Emission (NDE), Industrial Soot Emission (SE), Liquefied Petroleum Gas Supply (LPGS), Annual Electricity Consumption (AEC), Gas Supply (GS), Luminous remote sensing image brightness values (LRS), Water Supply (WS)).

the experiment was 0.736 and passed Bartlett's test of sphericity ($p<0.01$). This indicates a correlation between the variables and is suitable for indicator construction using the PCA method.

Table 1
Total Variance Explained

Component	Initial Eigenvalues			Extraction Sums of Squared Loadings			Rotation Sums of Squared Loadings		
	Total	Variance %	Cumulative %	Total	Variance %	Cumulative %	Total	Variance %	Cumulative %
1	4.887	34.909	34.909	4.887	**34.909**	34.909	4.555	32.533	32.533
2	3.739	26.705	61.614	3.739	**26.705**	61.614	2.767	19.762	52.294
3	2.228	15.916	77.530	2.228	**15.916**	77.530	2.690	19.218	71.512
4	1.157	8.264	85.794	1.157	**8.264**	**85.794**	1.999	14.281	85.794
5	0.566	4.043	89.837						
6	0.443	3.167	93.004						
7	0.345	2.468	95.471						
8	0.174	1.245	96.716						
9	0.160	1.142	97.858						
10	0.091	0.651	98.509						
11	0.067	0.482	98.991						
12	0.060	0.425	99.417						
13	0.043	0.309	99.726						
14	0.038	0.274	100.000						

Extraction Method: Principal Component Analysis.

We extracted the indicators with loadings greater than 0.7 in the rotated principal component matrix as the constituent indicators of the corresponding principal component indicators. As shown in Table 2, we selected data factors with loadings greater than 0.7, and four city carbon emission driven principal component indicators were constructed. These four principal component indicators represent, respectively, carbon emission driven by the improvement of urban residents' living standards (economic driven, including PBR, LPGS, AEC, GS, LRS, WS), carbon emission driven by the insufficient environmental and ecological carrying capacity of the city (environmental driven, including WR, CS, NPP), carbon emission driven by the industrial development of the city (industrial driven, including SDE, NDE, SE), and carbon emission driven by the insufficient potential of clean energy development (resource driven, including WEP and SEP).

Table 2
Rotated Component Matrix

Index	Component			
	1	2	3	4
Water Resource (WR)	-0.035	**0.958**	-0.034	-0.035
Wind energy potential (WEP)	0.006	0.152	-0.091	**0.962**
Solar energy potential (SEP)	0.031	0.427	-0.097	**0.876**
Carbon Sequestration (CS)	0.032	**0.921**	-0.035	0.336
Net Primary Productivity (NPP)	0.072	**0.874**	-0.056	0.378
Public Budget Revenue (PBR)	**0.952**	0.006	0.059	-0.004
Sulphur Dioxide Emission (SDE)	0.061	-0.146	**0.873**	-0.108
Nitrogen Dioxide Emission (NDE)	0.183	0.024	**0.942**	-0.067
Industrial Soot Emission (SE)	0.039	-0.003	**0.874**	-0.015
Liquefied Petroleum Gas Supply (LPGS)	**0.747**	-0.006	-0.109	0.110
Annual Electricity Consumption (AEC)	**0.840**	0.051	0.420	-0.092
Gas Supply (GS)	**0.827**	0.021	0.012	-0.063
Luminous remote sensing area image brightness values (LRS)	**0.895**	0.064	0.243	-0.015
Water Supply (WS)	**0.923**	-0.037	0.046	0.087

Note: Rotation converged in 5 iterations.

Table 3 shows the principal component coefficient scores we calculated. Based on the 14 indicator values of cities multiplied by the scores of different principal components, we can obtain the evaluation scores of different sub-indicators F for 197 cities. A higher score of a subindex F of a city $city_i$ means that this index F is the main causative factor of carbon emission in the city. In addition, we calculate the variance contribution of each principal component according to Equation 3 to obtain the composite index CI of carbon emission of the city.

The first column of Figure. 6 shows the spatial distribution of each sub-indicator ($F_1 - F_4$) we constructed, the second column shows the calculation results of spatial autocorrelation of each indicator. The third column shows the calculation results of the local Moran index (confidence level $p < 0.05$), which divides all cities into H-H class (cities around cities with high indicator F also have higher indicator F), L-L class (cities with low indicators F surround cities with low indicators F), i.e., the spatial clustering of carbon emission drivers F is formed. There are also spatial dispersions of carbon emission drivers F, i.e., H-L class (cities around cities with high indicator F have lower indicator F), and L-H class (cities around cities with low indicator F have higher indicator F).

Cities with economically driven carbon emissions are mainly concentrated in developed coastal regions, with a Moran index of 0.189 (subplots a,f,k). Large cities such as Beijing, Shanghai and Guangzhou have higher carbon emissions, and the surrounding cities also have higher carbon emissions. These cities have more developed economies and drive the economic growth of the surrounding cities. The residents' income and vehicle ownership are higher, so they are typical cities where the economy and living standards drive carbon emissions. The H-L region is mainly concentrated in inland provincial capitals, such as Kunming, Xi'an, Lanzhou, Nanning, Changsha, etc. The typical characteristics of these cities are that their economic development level is among the highest in the province, and their residents' energy consumption far exceeds that of the neighbouring cities. Such cities with economically driven carbon emissions should, in particular, set more stringent fuel consumption standards for vehicles, consider developing nuclear

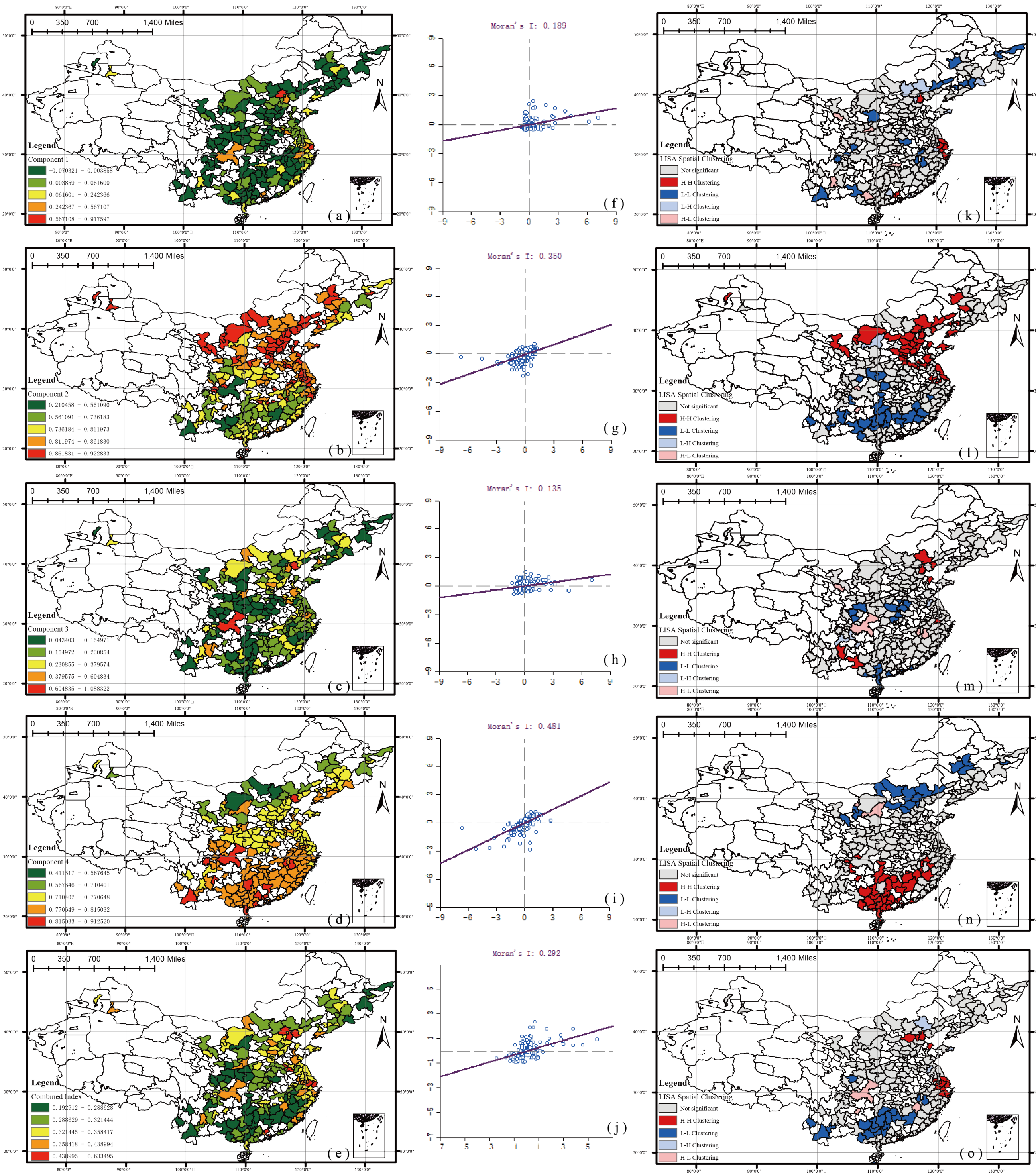

Figure 6: Spatial distribution and spatial autocorrelation calculation results of urban carbon emission drivers ($p < 0.05$, from top to bottom, F_1: economy-driven indicator, F_2: environment-driven indicator, F_3: industry-driven indicator, F_4: resource-driven indicator and CI:composite index; from left to right, respectively, indicator distribution, Moran index, and LISA test results. The x-axis of the Moran index represents the observed values for each principal component and the y-axis represents the spatial lag of observed values.)

Table 3
Component Score Coefficient Matrix

Index	Component			
	1	2	3	4
Water Resource (WR)	-0.017	**0.461**	-0.011	-0.279
Wind energy potential (WEP)	-0.010	-0.184	0.047	**0.596**
Solar energy potential (SEP)	-0.006	-0.032	0.036	**0.464**
Carbon Sequestration (CS)	-0.007	**0.344**	0.016	-0.023
Net Primary Productivity (NPP)	0.004	**0.310**	0.008	0.015
Public Budget Revenue (PBR)	**0.219**	-0.007	-0.051	-0.016
Sulphur Dioxide Emission (SDE)	-0.050	-0.038	**0.344**	0.042
Nitrogen Dioxide Emission (NDE)	-0.030	0.030	**0.367**	0.028
Industrial Soot Emission (SE)	-0.059	0.005	**0.354**	0.067
Liquefied Petroleum Gas Supply (LPGS)	**0.182**	-0.042	-0.094	0.053
Annual Electricity Consumption (AEC)	**0.165**	0.040	0.099	-0.053
Gas Supply (GS)	**0.194**	0.016	-0.065	-0.061
Luminous remote sensing area image brightness values (LRS)	**0.191**	0.024	0.029	-0.021
Water Supply (WS)	**0.212**	-0.052	-0.046	0.056

power or purchasing "wind power" and "hydropower" from neighbouring cities, and vigorously promote natural gas to replace energy-intensive coal consumption ("coal to gas").

Cities with environmentally driven carbon emissions are mainly concentrated in the North (the primary measure is negative indicators such as plant carbon sinks), with a Moran index of 0.350 (subplots b,g,l). This phenomenon can be clearly explained according to the NPP variation diagram in the Appendix. Northern cities have less light and heat resources than southern cities, and plants are scarce and cannot be evergreen in all seasons, which is not conducive to the formation of plant carbon sinks. In contrast, southern cities and cities with more forested mountains form large L-L areas. When formulating emission reduction policies, such cities with environment-driven carbon emissions should focus on ecological protection and afforestation to increase terrestrial plant carbon sinks.

Cities with industry-driven carbon emissions are mainly concentrated in cities with abundant resources and developed secondary industries such as iron and steel (Tangshan City, the largest crude steel-producing city in China with a population of less than 8 million and annual steel production comparable to that of the United States), with a Moran index of 0.135 (subplot c,h,m). Such cities with industry-driven carbon emissions should focus on energy efficiency, accelerate industrial upgrading, eliminate high-energy and high-polluting enterprises, and shift from "bigger" industries to "finer" industries when formulating emission reduction policies.

Cities with resource-driven carbon emissions (the main measures are negative indicators such as solar and wind energy, as shown in Figure S8 a,d) have a Moran index of 0.481 (subfigure d,i,n). Northern cities near the Mongolian plateau have much clean energy and potential for further development, forming a sizeable L-L region. Such cities with resource-driven carbon emissions are mainly concentrated in southern China, where the potential for clean energy development is low. Instead of blindly building inefficient clean energy power plants, consideration should be given to starting from the aspect of plant carbon sinks when formulating emission reduction policies and purchasing resources from energy-rich regions to meet the needs of urban development.

We finally show the distribution of carbon emissions as a composite indicator, and we can see a significant spatial dependence of carbon emissions (subplots e,j,o). H-H regions are mainly concentrated in the Bohai Rim city cluster around Beijing and the Yangtze River Delta city cluster around Shanghai. These regions are the most economically developed in China, indicating that the most crucial driver of China's current carbon emissions is still economic development. As shown in Table 1, the economic-driven principal component can explain more than 30% of carbon emissions. It can be expected that total CO_2 emissions will still rise in the coming years as China's economy grows.

This section summarises the spatial distribution of the four main drivers of carbon emissions - economic, environmental, industrial and resource. The results show two apparent spatial differences. The first is the difference between developed cities-less developed cities and the difference between industrialized cities-less industrialized & de-industrialized cities. Developed regions are emitting more CO_2, creating clear spatial hotspots (Figure 6). Similarly, industrialized cities consume more fossil energy, and carbon pricing policies help to compensate for the lack of spatial justice resulting from such economic and industrial differences. The second clear difference is the North-South divide in China, with cities in the South generally having insufficient clean energy development potential and abundant plant carbon sinks, while the opposite is true for cities in the North. The implementation of a carbon trading market could compensate for this imbalance in the spatial distribution of resources, allowing residents of the North and the South to enjoy equal and fair rights to development.

4.3. Model Fitting and Spatial Dependence of Urban Carbon Emissions

Table 4 and Table 5 show the fitting results of the SEM and OLS models, which fit of carbon emission indicators with the actual carbon emissions of the city, respectively. It can be seen that the fitting effect of the SEM model ($R^2 = 0.755$) is more significant than that of the OLS model ($R^2 = 0.722$), which suggests that carbon emission has spatial dependence. The F_2 indicator (environment-driven, mainly plant carbon sinks) in the OLS model did not pass the p test, which indicates that there are significant spatial differences in plant carbon sinks in the north and south regions of China. The results also confirm the conclusions in the section 4.2.

Table 4
Ordinary least squares model fitting results

Variable	Coefficient	Std.Error	z-value	Probability
Constant	0.449	0.124	3.621	0.000
F_1	0.751	0.045	16.735	0.000
F_2	-0.007	0.069	-0.100	**0.920**
F_3	0.572	0.045	12.833	0.000
F_4	-0.569	0.116	-4.917	0.000

Note1: Adjusted R-squared of the fit = 0.722.
Note2: If Probability<0.001 then Probability=0.

Table 5
Spatial error model fitting results

Variable	Coefficient	Std.Error	z-value	Probability
CONSTANT	0.619	0.123	5.016	0.000
F_1	0.736	0.044	16.770	0.000
F_2	-0.143	0.067	-2.113	0.030
F_3	0.573	0.044	13.061	0.000
F_4	-0.652	0.122	-5.325	0.000
LAMBDA	0.353	0.078	4.543	0.000

Note1: R-squared of the fit = 0.755.
Note2: If Probability<0.001 then Probability=0.

In addition, the linear regression model, Robust LM (error) is largely significant ($p = 0.060$), while Robust LM (lag) is insignificant ($p = 0.213$). The general OLS model does not meet our needs, while the SEM model passes the significance test for each parameter. As can be seen in Table 5, F_1 (economy-driven) and F_3 (industry-driven) have a very positive effect on urban carbon emissions.

Finally, we plotted the city scores of the urban carbon emissions composite index (CI) (Figure 7). It, unlike considering only urban carbon emissions (Figure 4 a), also takes into account a city's ability of carbon sequestration and decarbonization. The results show that the CI indices of first-tier cities such as Shanghai, Beijing, Suzhou, Guangzhou and Shenzhen (all with a GDP of over US$300 billion) are very high (Level1), while the CO_2 emissions of Beijing, Guangzhou and Shenzhen are not the highest (Figure 4 a,Level2). It illustrates the great contradiction between the tight land resources of regions and the development of a green economy. Developed cities tend to shift downstream industries to neighbouring regions due to the scarcity of land resources (Tian et al., 2019). The results of the LISA analysis of the CI (Figure 6) also illustrate this spatial dependence condition. In addition to the North-South and Affluence-Poverty

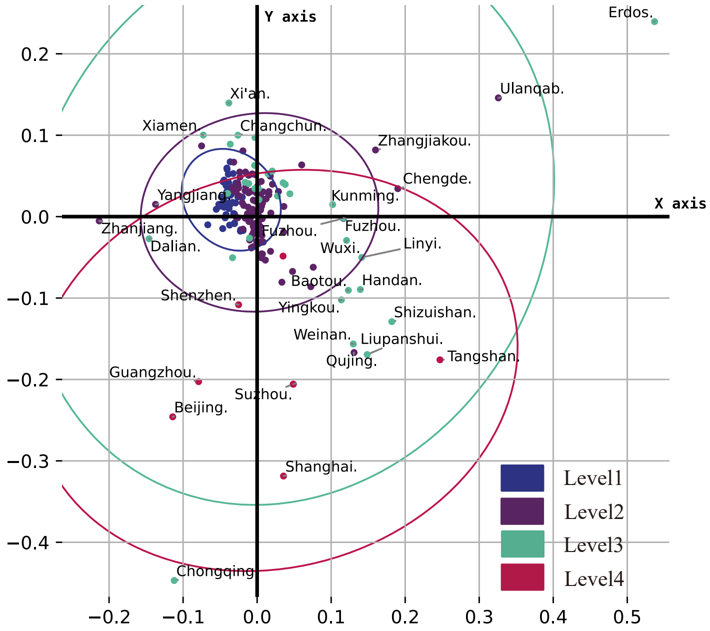

Figure 7: Distribution of CI indicators for cities considering carbon sequestration and substitution capacity (using the natural breakpoint classification, the CI indicators are categorised into 4 levels from low to high)

differences already discussed, there is also some spatial spillover from high-carbon emission cities, and thus its impact extends to surrounding areas.

5. Conclusion and Policy Implications

We find that a carbon pricing policy would have a positive effect on bridging the gap between rich and poor. Under the premise of carbon neutrality, China will generate a large scale carbon trading market, as well as generate US $153 billion of capital flows across cities, which will have an important impact on the location of energy-intensive enterprises and the economic distribution pattern of the country. Afterwards, we classified nearly 200 cities in China into four types of carbon emissions, namely, economy-driven, environment-driven, industry-driven and resource-driven, based on 14 carbon-related urban indicators, and proposed corresponding solutions.

Spatial justice requires the provision of equal and free development opportunities, the core of which is to balance efficiency and equity and to maximize the overall and long-term benefits. Carbon pricing policies, on the other hand, help to shift the damage or losses caused by greenhouse gas emissions back to the responsible parties who can reduce them. As represented by China, developing countries often tend to develop with the aim of economic growth and profit maximization. The less developed cities provide industrial workers, natural resources and consumer markets for the developed cities, and the excessive greenhouse gas emissions of developed cities exacerbate this spatial inequality (the inequality also exists between developed and developing countries).

There are still some limitations in our study, as there are other sources of carbon emissions in the city than the main ones considered in this paper, and we have not taken into account the Carbon Capture and Storage technology. The implications of carbon pricing are far-reaching and may even change existing economic development patterns and energy distribution&consumption patterns, and its impact on spatial justice is multifaceted and multi-layered. With the gradual implementation of the carbon market in the world, its impact needs to be further observed.

Declaration of competing interest

The authors declare that they have no known competing financial interests or personal relationships that could have appeared to influence the work reported in this paper.

Acknowledgements

The numerical calculations in this paper have been done on the super computing system in the Super computing Center of Wuhan University. The authors gratefully acknowledge financial support from China Scholarship Council.

This research was supported by the National Key R&D Program (2018YFB2100500), National Nature Science Foundation of China (41971351, 41771422), and China Scholarship Council (202106270048).

References

Acheampong, A.O., Opoku, E.E.O., Dzator, J.. Does democracy really improve environmental quality? empirical contribution to the environmental politics debate. Energy Economics 2022;:105942.

Amri, F.. The relationship amongst energy consumption (renewable and non-renewable), and gdp in algeria. Renewable and Sustainable Energy Reviews 2017;76:62–71.

Avila, S.. Environmental justice and the expanding geography of wind power conflicts. Sustainability Science 2018;13(3):599–616.

Brent, A.C., Hinkley, J., Burmester, D., Rayudu, R.. Solar atlas of new zealand from satellite imagery. Journal of the Royal Society of New Zealand 2020;50(4):572–583.

Caineng, Z., Songqi, P., Qun, H.. On the connotation, challenge and significance of china's "energy independence" strategy. Petroleum Exploration and Development 2020;47(2):449–462.

Chao, Y.. The methodology on spatial justice and newtype urbanization. Geographical Research 2019;38(1):146–154.

Chen, J., Gao, M., Cheng, S., Hou, W., Song, M., Liu, X., Liu, Y., Shan, Y.. County-level co 2 emissions and sequestration in china during 1997–2017. Scientific Data 2020a;7(1):1–12.

Chen, N., Zhang, Y., Du, W., Li, Y., Chen, M., Zheng, X.. Ke-cnn: A new social sensing method for extracting geographical attributes from text semantic features and its application in wuhan, china. Computers, Environment and Urban Systems 2021;88:101629.

Chen, W., Shen, Y., Wang, Y., Wu, Q.. The effect of industrial relocation on industrial land use efficiency in china: A spatial econometrics approach. Journal of Cleaner Production 2018;205:525–535.

Chen, X., Lin, B.. Towards carbon neutrality by implementing carbon emissions trading scheme: Policy evaluation in china. Energy Policy 2021;157:112510.

Chen, Z., Yuan, X.C., Zhang, X., Cao, Y.. How will the chinese national carbon emissions trading scheme work? the assessment of regional potential gains. Energy Policy 2020b;137:111095.

Cheng, J., Mao, C., Huang, Z., Hong, J., Liu, G.. Implementation strategies for sustainable renewal at the neighborhood level with the goal of reducing carbon emission. Sustainable Cities and Society 2022;:104047.

Dallaire, C.O., Lehner, B., Sayre, R., Thieme, M.. A multidisciplinary framework to derive global river reach classifications at high spatial resolution. Environmental Research Letters 2019;14(2):024003.

Fang, J., Yu, G., Liu, L., Hu, S., Chapin, F.S.. Climate change, human impacts, and carbon sequestration in china. Proceedings of the National Academy of Sciences 2018;115(16):4015–4020.

Gruber, K., Klöckl, C., Regner, P., Baumgartner, J., Schmidt, J.. Assessing the global wind atlas and local measurements for bias correction of wind power generation simulated from merra-2 in brazil. Energy 2019;189:116212.

Guan, D., Meng, J., Reiner, D.M., Zhang, N., Shan, Y., Mi, Z., Shao, S., Liu, Z., Zhang, Q., Davis, S.J.. Structural decline in china's co 2 emissions through transitions in industry and energy systems. Nature Geoscience 2018;11(8):551–555.

Guan, D., Shan, Y., Liu, Z., He, K.. Performance assessment and outlook of china's emission-trading scheme. Engineering 2016;2(4):398–401.

Hernández, C., Barraza, R., Saez, A., Ibarra, M., Estay, D.. Potential map for the installation of concentrated solar power towers in chile. Energies 2020;13(9):2131.

jiemin, H., chen, W.. The impact of private sector energy investment, innovation and energy consumption on china's carbon emissions. Renewable Energy 2022;195:1291–1299. URL: https://www.sciencedirect.com/science/article/pii/S0960148122009715. doi:https://doi.org/10.1016/j.renene.2022.06.131.

Khosravi, A., Olkkonen, V., Farsaei, A., Syri, S.. Replacing hard coal with wind and nuclear power in finland-impacts on electricity and district heating markets. Energy 2020;203:117884.

Li, L., Ye, F., Li, Y., Chang, C.T.. How will the chinese certified emission reduction scheme save cost for the national carbon trading system? Journal of environmental management 2019;244:99–109.

Li, R., Li, L., Wang, Q.. The impact of energy efficiency on carbon emissions: Evidence from the transportation sector in chinese 30 provinces. Sustainable Cities and Society 2022;:103880URL: https://www.sciencedirect.com/science/article/pii/S2210670722002062. doi:https://doi.org/10.1016/j.scs.2022.103880.

Linke, S., Lehner, B., Dallaire, C.O., Ariwi, J., Grill, G., Anand, M., Beames, P., Burchard-Levine, V., Maxwell, S., Moidu, H., et al. Global hydro-environmental sub-basin and river reach characteristics at high spatial resolution. Scientific data 2019;6(1):1–15.

Liu, H., Fan, J., Zhou, K., Wang, Q.. Exploring regional differences in the impact of high energy-intensive industries on co 2 emissions: evidence from a panel analysis in china. Environmental Science and Pollution Research 2019;26(25):26229–26241.

Liu, J., Chen, N., Chen, Z., Xu, L., Du, W., Zhang, Y., Wang, C.. Towards sustainable smart cities: Maturity assessment and development pattern recognition in china. Journal of Cleaner Production 2022;370:133248.

Liu, J.Y., Woodward, R.T., Zhang, Y.J.. Has carbon emissions trading reduced pm2. 5 in china? Environmental Science & Technology 2021;.

Londono-Pulgarin, D., Cardona-Montoya, G., Restrepo, J.C., Munoz-Leiva, F.. Fossil or bioenergy? global fuel market trends. Renewable and Sustainable Energy Reviews 2021;143:110905.

Van der Maaten, L., Hinton, G.. Visualizing data using t-sne. Journal of machine learning research 2008;9(11).

de Mendonca, H.V., Assemany, P., Abreu, M., Couto, E., Maciel, A.M., Duarte, R.L., dos Santos, M.G.B., Reis, A.. Microalgae in a global world: New solutions for old problems? Renewable Energy 2021;165:842–862.

Mikovits, C., Schauppenlehner, T., Scherhaufer, P., Schmidt, J., Schmalzl, L., Dworzak, V., Hampl, N., Sposato, R.G.. A spatially highly resolved ground mounted and rooftop potential analysis for photovoltaics in austria. ISPRS International Journal of Geo-Information 2021;10(6). URL: https://www.mdpi.com/2220-9964/10/6/418. doi:10.3390/ijgi10060418.

Nabernegg, S., Bednar-Friedl, B., Muñoz, P., Titz, M., Vogel, J.. National policies for global emission reductions: Effectiveness of carbon emission reductions in international supply chains. Ecological Economics 2019;158:146–157.

Opeyemi, B.M.. Path to sustainable energy consumption: The possibility of substituting renewable energy for non-renewable energy. Energy 2021;228:120519.

Ou, J., Liu, X., Liu, P., Liu, X.. Evaluation of luojia 1-01 nighttime light imagery for impervious surface detection: A comparison with npp-viirs nighttime light data. International Journal of Applied Earth Observation and Geoinformation 2019;81:1–12.

Ouyang, Z., Song, C., Zheng, H., Polasky, S., Xiao, Y., Bateman, I.J., Liu, J., Ruckelshaus, M., Shi, F., Xiao, Y., et al. Using gross ecosystem product (gep) to value nature in decision making. Proceedings of the National Academy of Sciences 2020;117(25):14593–14601.

Pravitasari, A.E., Rustiadi, E., Mulya, S.P., Fuadina, L.N.. Developing regional sustainability index as a new approach for evaluating sustainability performance in indonesia. Environ Ecol Res 2018;6:157–168.

Qiu, T., Wang, L., Lu, Y., Zhang, M., Qin, W., Wang, S., Wang, L.. Potential assessment of photovoltaic power generation in china. Renewable and Sustainable Energy Reviews 2022;154:111900.

Ristic, B., Mahlooji, M., Gaudard, L., Madani, K.. The relative aggregate footprint of electricity generation technologies in the european union (eu): A system of systems approach. Resources, Conservation and Recycling 2019;143:282–290.

Schubert, P., Kirchner, M.. Ellipse area calculations and their applicability in posturography. Gait & Posture 2014;39(1):518–522.

Semieniuk, G., Yakovenko, V.M.. Historical evolution of global inequality in carbon emissions and footprints versus redistributive scenarios. Journal of Cleaner Production 2020;264:121420.

Shan, Y., Guan, D., Zheng, H., Ou, J., Li, Y., Meng, J., Mi, Z., Liu, Z., Zhang, Q.. China co 2 emission accounts 1997–2015. Scientific data 2018;5(1):1–14.

Shan, Y., Huang, Q., Guan, D., Hubacek, K.. China co 2 emission accounts 2016–2017. Scientific data 2020;7(1):1–9.

Soja, E.. The city and spatial justice. Justice spatiale/Spatial justice 2009;1(1):1–5.

Soja, E.W.. Seeking spatial justice. volume 16. U of Minnesota Press, 2013.

Sovacool, B.K., Burke, M., Baker, L., Kotikalapudi, C.K., Wlokas, H.. New frontiers and conceptual frameworks for energy justice. Energy Policy 2017;105:677–691.

Sovacool, B.K., Lipson, M.M., Chard, R.. Temporality, vulnerability, and energy justice in household low carbon innovations. Energy Policy 2019;128:495–504.

Steckel, J.C., Dorband, I.I., Montrone, L., Ward, H., Missbach, L., Hafner, F., Jakob, M., Renner, S.. Distributional impacts of carbon pricing in developing asia. Nature Sustainability 2021;4(11):1005–1014.

Sun, H., Wang, E., Li, X., Cui, X., Guo, J., Dong, R.. Potential biomethane production from crop residues in china: Contributions to carbon neutrality. Renewable and Sustainable Energy Reviews 2021;148:111360.

Sun, Y., Zhao, T., Xia, L.. Spatial-temporal differentiation of carbon efficiency and coupling coordination degree of chinese county territory and obstacles analysis. Sustainable Cities and Society 2022;76:103429.

Tian, Y., Jiang, G., Zhou, D., Ding, K., Su, S., Zhou, T., Chen, D.. Regional industrial transfer in the jingjinji urban agglomeration, china: An analysis based on a new "transferring area-undertaking area-dynamic process" model. Journal of Cleaner Production 2019;235:751–766.

Uwayezu, E., De Vries, W.T.. Indicators for measuring spatial justice and land tenure security for poor and low income urban dwellers. Land 2018;7(3):84.

Vaninsky, A.. Multiobjective restructuring aimed at green economic growth. Environment Systems and Decisions 2021;41(1):110–130.

Wang, J., Sun, R., Zhang, H., Xiao, Z., Zhu, A., Wang, M., Yu, T., Xiang, K.. New global musyq gpp/npp remote sensing products from 1981 to 2018. IEEE Journal of Selected Topics in Applied Earth Observations and Remote Sensing 2021a;.

Wang, M., Wang, Y., Chen, L., Yang, Y., Li, X.. Carbon emission of energy consumption of the electric vehicle development scenario. Environmental Science and Pollution Research 2021b;28(31):42401–42413.

Wang, Q., Su, M.. Drivers of decoupling economic growth from carbon emission–an empirical analysis of 192 countries using decoupling model and decomposition method. Environmental Impact Assessment Review 2020;81:106356.

Wang, S., Xie, Z., Wu, R.. Examining the effects of education level inequality on energy consumption: Evidence from guangdong province. Journal of Environmental Management 2020;269:110761.

Wang, S., Zhang, X., Chen, N., Wang, W.. Classifying diurnal changes of cyanobacterial blooms in lake taihu to identify hot patterns, seasons and hotspots based on hourly goci observations. Journal of Environmental Management 2022a;310:114782.

Wang, Y., Niu, Y., Li, M., Yu, Q., Chen, W.. Spatial structure and carbon emission of urban agglomerations: Spatiotemporal characteristics and driving forces. Sustainable Cities and Society 2022b;78:103600.

Wu, R., Xie, Z.. Identifying the impacts of income inequality on co2 emissions: empirical evidences from oecd countries and non-oecd countries. Journal of Cleaner Production 2020;277:123858.

Xing, Z., Jiao, Z., Wang, H.. Carbon footprint and embodied carbon transfer at city level: A nested mrio analysis of central plain urban agglomeration in china. Sustainable Cities and Society 2022;:103977.

Yan, D., Lei, Y., Li, L., Song, W.. Carbon emission efficiency and spatial clustering analyses in china's thermal power industry: Evidence from the provincial level. Journal of Cleaner Production 2017;156:518–527.

Yang, J., Zhang, W., Zhao, D., Zhao, C., Yuan, J.. What can china learn from the uk's transition to a low-carbon power sector? a multi-level perspective. Resources, Conservation and Recycling 2022;179:106127.

Yue, X., Peng, M.Y.P., Anser, M.K., Nassani, A.A., Haffar, M., Zaman, K.. The role of carbon taxes, clean fuels, and renewable energy in promoting sustainable development: How green is nuclear energy? Renewable Energy 2022;193:167–178.

Zhang, F., Deng, X., Phillips, F., Fang, C., Wang, C.. Impacts of industrial structure and technical progress on carbon emission intensity: Evidence from 281 cities in china. Technological Forecasting and Social Change 2020;154:119949.

Zhang, L., Li, S., Nie, Q., Hu, Y.. A two-stage benefit optimization and multi-participant benefit-sharing strategy for hybrid renewable energy systems in rural areas under carbon trading. Renewable Energy 2022a;189:744–761.

Zhang, X., Brandt, M., Tong, X., Ciais, P., Yue, Y., Xiao, X., Zhang, W., Wang, K., Fensholt, R.. A large but transient carbon sink from urbanization and rural depopulation in china. Nature Sustainability 2022b;:1–8.

Zhang, Y., Chen, N., Du, W., Li, Y., Zheng, X.. Multi-source sensor based urban habitat and resident health sensing: A case study of wuhan, china. Building and Environment 2021a;198:107883.

Zhang, Y., Chen, Z., Zheng, X., Chen, N., Wang, Y.. Extracting the location of flooding events in urban systems and analyzing the semantic risk using social sensing data. Journal of Hydrology 2021b;603:127053.

Zhang, Y., Zhang, F., Chen, N.. Migratable urban street scene sensing method based on vision language pre-trained model. International Journal of Applied Earth Observation and Geoinformation 2022c;113:102989.

Zhang, Y., Zheng, X., Helbich, M., Chen, N., Chen, Z.. City2vec: Urban knowledge discovery based on population mobile network. Sustainable Cities and Society 2022d;:104000.

Zhang, Z., Hu, G., Mu, X., Kong, L.. From low carbon to carbon neutrality: A bibliometric analysis of the status, evolution and development trend. Journal of Environmental Management 2022e;322:116087.

Zhao, X., Ma, X., Chen, B., Shang, Y., Song, M.. Challenges toward carbon neutrality in china: Strategies and countermeasures. Resources, Conservation and Recycling 2022;176:105959.

Zhao, X.g., Wu, L., Li, A.. Research on the efficiency of carbon trading market in china. Renewable and Sustainable Energy Reviews 2017;79:1–8.

Zhou, C., Wang, S., Wang, J.. Examining the influences of urbanization on carbon dioxide emissions in the yangtze river delta, china: Kuznets curve relationship. Science of the Total Environment 2019;675:472–482.

Zhu, B., Zhang, M., Huang, L., Wang, P., Su, B., Wei, Y.M.. Exploring the effect of carbon trading mechanism on china's green development efficiency: A novel integrated approach. Energy Economics 2020;85:104601.

6. Supplementary Material

Supplementary Material, Table S6

Summarizes the data sources for the variables mentioned above

Data name	Data Introduction	Data Source
Luminous remote sensing area image brightness values (LRS)	Luojia-01 (Ou et al., 2019)	hbeos.org.cn
NPP/GPP	Global MuSyQ GPP/NPP remote sensing products (Wang et al., 2021a)	doi.org/10.5281/zenodo.3996814
Solar energy potential (SEP)	Global Solar Atlas 2.0 (Brent et al., 2020)	globalsolaratlas.info/map
Wind energy potential (WEP)	Global Wind Atlas (Gruber et al., 2019)	globalwindatlas.info
Carbon Sequestration (CS)	China CO_2 emission accounts (Shan et al., 2020)	doi.org/10.6084/m9.figshare.11793816.v2
Administrative divisions and standard maps of China	National Geomatics Center of China	www.ngcc.cn/ngcc
Other city indicators	China City statistical yearbooks or product data generated based on it	stats.gov.cn/tjsj/ndsj

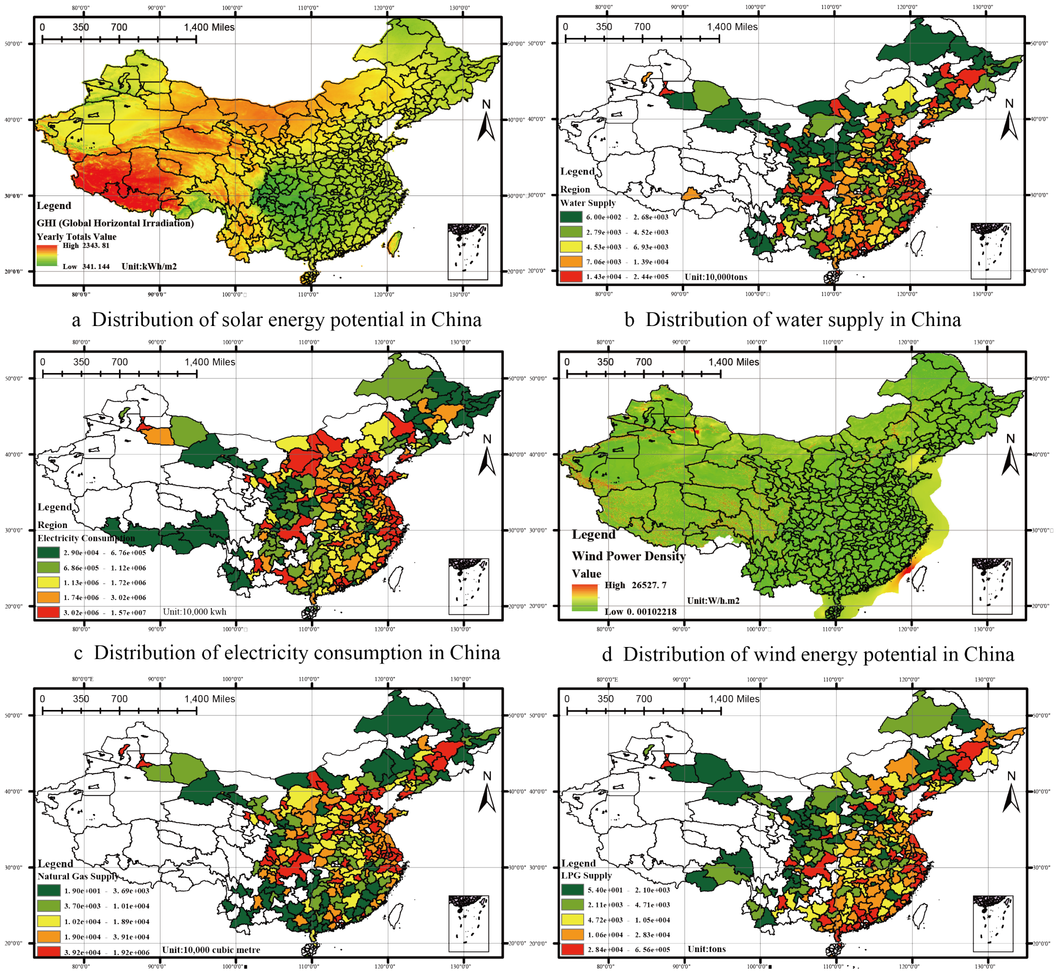

a Distribution of solar energy potential in China

b Distribution of water supply in China

c Distribution of electricity consumption in China

d Distribution of wind energy potential in China

e Distribution of natural gas supply in China

f Distribution of LPG supply in China

Supplementary Material, Figure S8: Spatial distribution of many indicators

Supplementary Material, Table S7
Changes in urban GDP per capita under the premise of carbon neutrality and carbon trading

City	Population (million)	Carbon Emission (million ton)	PerGDP (thousand yuan)	PerCarbonTax (thousand yuan)	NetPerGDP (thousand yuan)
Beijing	13.680	60.086	140.211	0.676	139.535
Tianjin	10.660	150.048	120.711	3.308	117.403
Shijiazhuang	9.770	94.952	55.723	2.136	53.587
Tangshan	7.570	102.060	87.855	2.817	85.038
Qinhuangdao	2.990	31.530	52.380	1.512	50.868
Handan	10.540	77.297	36.289	1.598	34.691
Xingtai	7.930	54.824	29.210	1.393	27.817
Baoding	12.040	85.810	31.057	1.254	29.803
Zhangjiakou	2.280	35.729	34.661	-2.205	36.866
...	...	...	...	...	...
Cangzhou	7.800	79.754	48.562	2.171	46.391
Langfang	4.770	64.077	64.906	3.107	61.799
Hcngshui	4.550	33.726	34.898	1.443	33.455
Taiyuan	3.730	38.886	88.272	2.053	86.219
Datong	3.180	41.360	36.877	1.739	35.138
Yangquan	1.320	17.428	51.976	2.024	49.952
Changzhi	3.390	32.815	47.540	0.808	46.732
Jincheng	2.210	29.529	57.819	1.757	56.062
Shuozhou	1.630	22.369	59.914	1.429	58.485
Jinzhong	3.330	38.449	42.910	1.123	41.787

Note: One dollar is about 6 - 7 yuan. Simultaneous implementation of carbon pricing in all cities, establishing a national carbon trading market and the moderate development of clean energy.